Modified Silicon Anode for Improved Low-Temperature Performance of Lithium-Ion Batteries

Jason A. Mennel
Department of Chemical and Materials Engineering,
University of Nevada, Reno,
Reno, NV 89557
e-mail: jmennel@unr.edu

Dev Chidambaram[1]
Department of Chemical and Materials Engineering,
University of Nevada, Reno,
Reno, NV 89557;
Nevada Institute for Sustainability,
University of Nevada, Reno,
Reno, NV 89557
e-mail: dcc@unr.edu

The shift away from fossil fuels for modern-day energy requirements has resulted in a higher demand for electric vehicles and has led to a critical role for lithium-ion batteries. Next-generation higher capacity electrode materials are needed to meet the demands of future electric vehicles. Lithium-ion batteries function optimally around room temperature (23 °C), but discharge capacity diminishes rapidly below 0 °C and significantly affects the population living in colder climates. Higher capacity electrode materials such as silicon need to be paired with new electrolytes that favor ideal low-temperature performance. This work pairs a typical nickel-rich lithium cathode with a modified silicon anode and a ternary carbonate/ester electrolyte to demonstrate improved discharge capacity at subzero temperature.
[DOI: 10.1115/1.4062163]

Keywords: NCA, carbonate, electrolyte, capacity, low temperature, batteries, electrochemical engineering, electrochemical storage, novel materials

1 Introduction

Nickel-rich transition metal oxides such as lithium nickel cobalt aluminum oxide ($LiNi_{0.8}Co_{0.15}Al_{0.05}O_2$; NCA) for cathode materials have allowed for higher capacity lithium-ion batteries to permeate the market in recent years [1]. Although various cathode chemistries have led to a significant growth in the production and adoption of electric vehicles, almost all of these batteries use graphite anodes. While higher capacity lithium-ion batteries are essential for longer range electric vehicles, batteries that retain such high capacity at subzero temperatures are also necessary for performance in colder climates. Populations that live in colder climates or colder winters currently face a diminishing battery capacity and subsequently vehicle range as typical lithium-ion cells start to lose capacity below about 0 °C (32 °F) [2]. It is also possible to improve overall battery capacity by changing the graphite anode, which has a theoretical capacity of 372 mAh/g, to higher capacity anode materials such as silicon (which has a theoretical capacity of 4200 mAh/g) [3,4]. Additionally, new-generation electrolytes are currently being investigated to address the loss in capacity at lower temperatures [5].

The main problem to address concerning silicon anodes is volume expansion [6], while those at lower temperatures include lithium plating, conductivity of lithium ions through the electrolyte, and desolvation of lithium from the electrolyte into the electrode [7–9]. Silicon anodes have been studied for years, with different methods to mitigate volume expansion such as synthesizing different Si structures or doping with various metals [10–12]. In this work, copper dichloride was used to improve the conductivity within the silicon electrode as well as to stabilize the electrode upon volume expansion, as stated in the previous literature [13]. Next-generation electrolytes have begun to include different organic groups such as esters for their low-melting temperatures, and various additives to improve lithium kinetics and desolvation behavior [14–16]. The use of silicon anodes, however, has not gained commercial footing, and much research is still needed before this next-generation high-capacity material is implemented commercially. To the best of our knowledge, a lithium-ion cell constructed with an NCA cathode, a copper-modified silicon anode, and a favorable electrolyte, has not been evaluated for its ability to provide improved low-temperature performance with higher capacity than traditional lithium-ion batteries using graphite anode, which this work demonstrates.

2 Materials and Methods

2.1 Electrode and Electrolyte Preparation. NCA, polyvinylidene fluoride, and Super C65 conductive carbon were mixed together in a 90:5:5 mass ratio and milled for 1 h to mix and reduce the particle size. The mixed powders were then added slowly to an appropriate amount of *N*-methyl-2-pyrrolidone as a solvent and stirred for 24 h for homogeneity. The slurry was cast onto the aluminum foil (10 μm) via a doctor blade and an automatic thick film coater. The casted foils were allowed to dry in a fume hood before placing in a vacuum oven at 120 °C for 12 h. These foils were then compressed to a thickness of 70 μm and used to punch disks of 12.7 mm with an electrode mass of 24.9 mg minus the aluminum foil, resulting in an electrode density of 2.46 g/cm^3.

To prepare anode disks, silicon nano-powder (Si, < 100 nm) and Super C65 carbon and copper dichloride ($CuCl_2$) were added to the slurry in a 76:14:8:2 mass ratio of silicon, binder, conductive carbon, and copper dichloride, respectively. The anode slurry was allowed to mix for 24 h for homogeneity and then cast onto the copper foil. This film was also dried similar to the cathode foil. The anode film was then heated at 700 °C for 15 min under argon. For the silicon–copper electrode described, previous literature has shown that a heat treatment step creates a Cu_3Si phase that helps stabilize the electrode upon lithium intercalation [17]. Disks of 12.7 mm were punched, and the thickness of the disks was measured to be 70 μm on average, while the electrode mass was recorded to be 2.7 mg minus the copper foil, resulting in an electrode density of 0.3 g/cm^3. Both cathode and anode disks were then transferred into a glove box that maintained water and oxygen levels at less than 1.0 ppm. The N/P ratio is 1.38 for these two electrodes.

A ternary carbonate electrolyte consisting of ethylene carbonate, ethyl methyl carbonate, and methyl propionate was used due to its improved low-temperature performance [18]. Cell membranes with 25 μm thickness were soaked in electrolyte before coin cell assembly, where 50 μL total of electrolyte was added per cell. CR 2032 coin cell casings, spacers, and springs were used as purchased. Coin cells were assembled and then crimped with an electric crimper, labeled for testing, and transferred out of the glove box.

2.2 Characterization. The surface morphology of the silicon anode discs was analyzed using an FEI Scios 2 Dual-Beam focused-ion beam/scanning electron microscope (SEM). A working distance of 7 mm and an accelerating voltage of 5 kV were used throughout the imaging process. Prior to cycling, the samples were investigated using a Rigaku SmartLab X-ray

[1]Corresponding author.
Manuscript received January 21, 2023; final manuscript received March 11, 2023; published online March 31, 2023. Assoc. Editor: Partha P. Mukherjee.

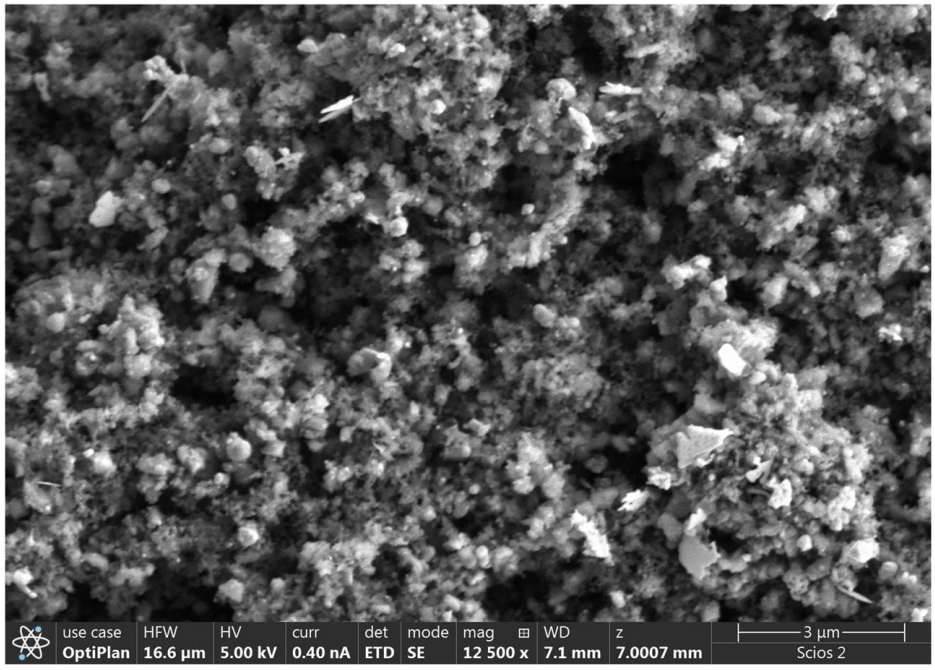

Fig. 1 SEM image showing even distribution of particle type and size throughout the surface of a silicon anode disc after the heat treatment step

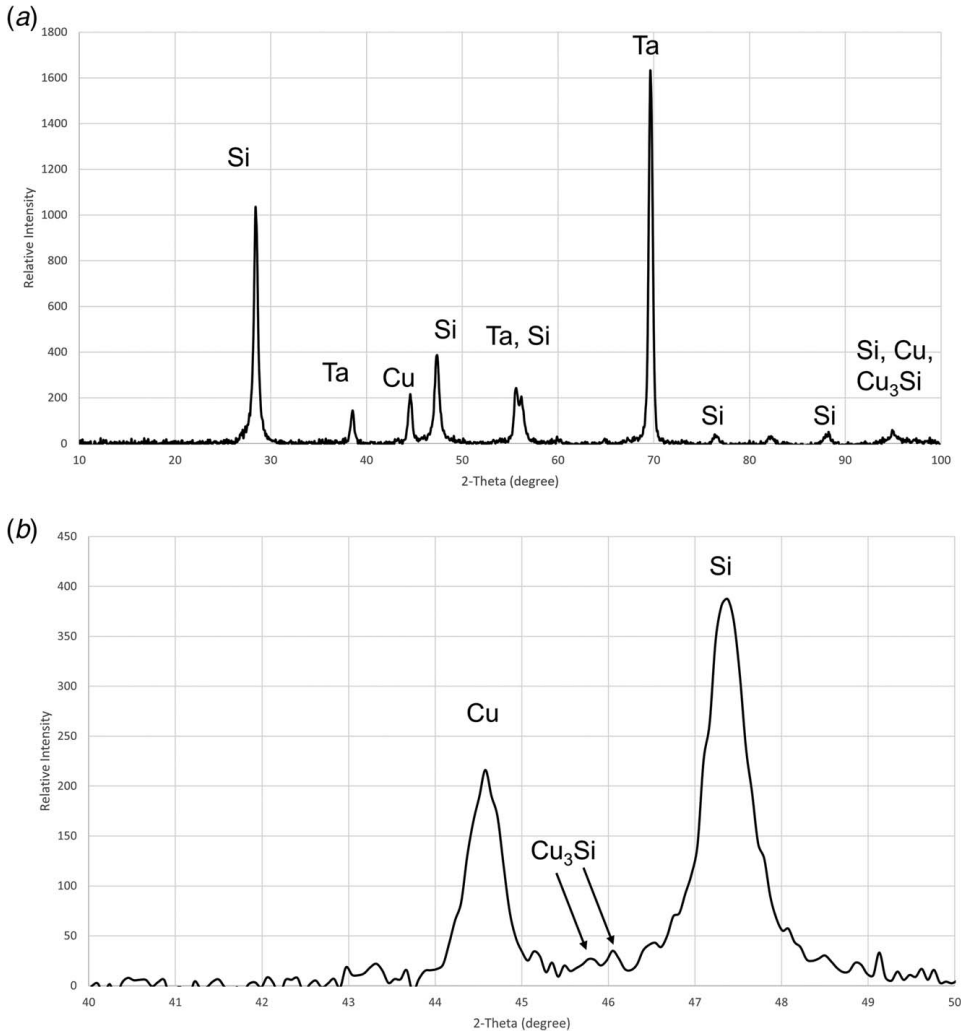

Fig. 2 (*a*) XRD pattern showing the various silicon, copper, and Cu_3Si phases and (*b*) section of the XRD pattern, indicating the specific Cu_3Si peaks as per JCPDS indexes

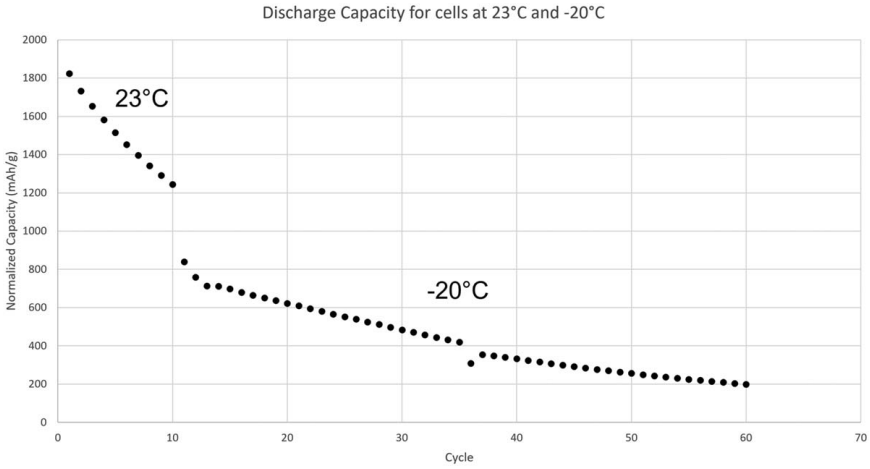

Fig. 3 NCA–Si cells that run for ten cycles at room temperature (23 °C) followed by 50 cycles at −20 °C

diffraction (XRD) to understand the lattice structure. To clearly see copper within the electrode versus interference from the copper foil, the exact same slurry was cast onto the tantalum foil at the same height. A scan from $2\theta = 10$ deg to 100 deg with a step size of 0.07 deg and a scan rate of 0.5 deg min^{-1} was collected for this sample. RIGAKU PDXL2 analysis software and JCPDS cards were used to help evaluate the XRD data.

2.3 Charge/Discharge Cycle Testing. An MTI multichannel battery analyzer rated for 5 V and 1 mA max was used for cycling studies. Cells were cycled with a hybrid constant-current constant-voltage test schedule between 2.0 V and 4.3 V at room temperature and at −20 °C. To establish a durable solid electrolyte interphase (SEI) layer, cells performed three room temperature cycles at a C/50 rate before beginning full testing at a C/10 rate. Full testing at room temperature commenced for ten cycles, followed by cycling at −20 °C in which cells were placed in an environmental chamber. Testing occurred at −20 °C for 50 cycles before concluding.

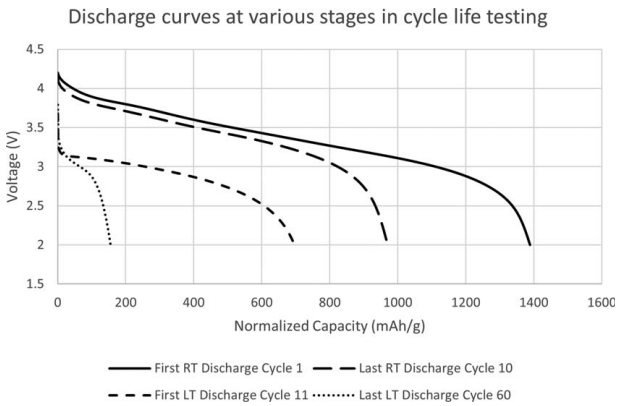

Fig. 4 Discharge curves showing capacity changes at first room temperature discharge, last room temperature discharge, first low-temperature discharge, and last low-temperature discharge. All cycles were run at the same C/10 discharge rate.

3 Results and Discussion

To observe the morphology characteristics of the silicon anode surface, SEM was conducted on punched electrodes after the heat treatment step. Figure 1 shows a homogenous surface with an average particle size between 100 nm and 500 nm. There are also porous channels of a few microns in diameter seen networking through the structure of the electrode material. This shows an even distribution of particle type and size for reliable cycle testing to be performed. To identify different phases in the crystal structure of the silicon anode before cycle testing, XRD was performed with casted anode slurry on tantalum foil after the heat treatment step, confirming the formation of a Cu_3Si phase that helps to stabilize the silicon electrode and increase conductivity as shown elsewhere [17]. This is corroborated by the JCPDS index 00-059-0262 and shown in Figs. 2(*a*) and 2(*b*).

The cycling data of the discharge reaction performed at room temperature (ten cycles) and −20 deg (50 cycles) are shown in Fig. 3. Several things are noticeable immediately, such as the much higher capacity of the silicon anode at room temperature (≈1400 mAh/g) compared to that of graphite and other lithium metal oxides (180 mAh/g–372 mAh/g, theoretical values). As is well known, the silicon anode does suffer from high initial capacity fade [10] and further loses significant capacity when transitioning from room temperature to −20 °C. However, it can be seen that discharge capacity fade decreases at a lower temperature, and the silicon electrodes are able to perform for 50 cycles while retaining approximately 150 mAh/g. This demonstrates important advantages in utilizing the common nickel-rich cathode paired with a higher capacity silicon anode and ternary carbonate/ester electrolyte to allow for higher capacity discharge at subzero temperatures. Discharge curves are also shown in Fig. 4 to further illustrate the capacity changes from initial to final room temperature conditions, and initial to final low-temperature conditions. Low temperatures drastically affect physical properties of electrolytes such as conductivity and viscosity. A decrease in ionic conductivity and an increase in viscosity of not only the electrolyte but also the SEI can increase the electrical polarization of the cell, resulting in lower operating voltages as seen in Fig. 4 [19]. These discharge curves reiterate the loss in capacity at low temperatures compared to room temperatures and also give a reference point from which to improve low-temperature performance of this chemistry via advanced electrode processing and electrolyte modification.

4 Conclusion

Incorporating high-capacity electrode materials into cells that cycle at subzero temperatures will help further increase the utilization and range of electric vehicles in colder regions of the world. The use of copper to alleviate volume expansion in the silicon anode, and a ternary carbonate/ester electrolyte helped to increase

the observable capacity witnessed throughout cycling. This resulted in approximately 1800 mAh/g upon first discharge at room temperature decreasing to about 1200 mAh/g at the tenth cycle. The capacity diminishes by 400 mAh/g to start discharge at −20 °C around 800 mAh/g, but exhibits a more gradual capacity fade at these lower temperatures. After 50 cycles at −20 °C, a capacity of 150 mAh/g is retained, showing still higher capacity retention than traditional lithium-ion cells would at room temperature. This work shows the feasibility of using higher capacity silicon anodes with transition metal additives and tuned electrolyte to allow for improved low-temperature performance. Further investigation will be needed to understand and decrease capacity fade and improve low-temperature capacity retention of this lithium-ion battery chemistry.

Acknowledgment

Dr. Ali Shaykhian served as the NASA technical monitor.

Funding Data

- The National Aeronautics and Space Administration (Award No. 80NSSC19M0152).

Conflict of Interest

There are no conflicts of interest.

Data Availability Statement

The datasets generated and supporting the findings of this article are obtainable from the corresponding author upon reasonable request.

References

[1] Kim, T., Song, W., Son, D. Y., Ono, L. K., and Qi, Y., 2019, "Lithium-Ion Batteries: Outlook on Present, Future, and Hybridized Technologies," J. Mater. Chem. A, **7**(7), pp. 2942–2964.

[2] Jaguemont, J., Boulon, L., and Dubé, Y., 2016, "A Comprehensive Review of Lithium-Ion Batteries Used in Hybrid and Electric Vehicles at Cold Temperatures," Appl. Energy, **164**, pp. 99–114.

[3] Farmakis, F., de Meatza, I., Subburaj, T., Tsiplakides, D., Argyropoulos, D. P., Balomenou, S., Landa-Medrano, I., Eguia-Barrio, A., Strataki, N., and Nestoridi, M., 2021, "Elucidation of the Influence of Operating Temperature in LiNi0.8Co0.15Al0.05O2/Silicon and LiNi0.8Co0.15Al0.05O2/Graphite Pouch Cells Batteries Cycle-Life Degradation," J. Energy Storage, **41**, p. 102989.

[4] Chen, X., Li, H., Yan, Z., Cheng, F., and Chen, J., 2019, "Structure Design and Mechanism Analysis of Silicon Anode for Lithium-Ion Batteries," Sci. China Mater., **62**(11), pp. 1515–1536.

[5] Jin, Y., Kneusels, N. J. H., Marbella, L. E., Castillo-Martínez, E., Magusin, P. C. M. M., Weatherup, R. S., Jónsson, E., Liu, T., Paul, S., and Grey, C. P., 2018, "Understanding Fluoroethylene Carbonate and Vinylene Carbonate Based Electrolytes for Si Anodes in Lithium-Ion Batteries With NMR Spectroscopy," J. Am. Chem. Soc., **140**(31), pp. 9854–9867.

[6] Liu, Y., Zhou, G., Liu, K., and Cui, Y., 2017, "Design of Complex Nanomaterials for Energy Storage: Past Success and Future Opportunity," Acc. Chem. Res., **50**(12), pp. 2895–2905.

[7] Arai, J., and Nakahigashi, R., 2017, "Study of Li Metal Deposition in Lithium Ion Battery During Low-Temperature Cycle Using In Situ Solid-State 7 Li Nuclear Magnetic Resonance," J. Electrochem. Soc., **164**(13), pp. A3403–A3409.

[8] Dong, X., Wang, Y. G., and Xia, Y., 2021, "Promoting Rechargeable Batteries Operated at Low Temperature," Acc. Chem. Res., **54**(20), pp. 3883–3894.

[9] Li, Q., Lu, D., Zheng, J., Jiao, S., Luo, L., Wang, C. M., Xu, K., Zhang, J. G., and Xu, W., 2017, "Li+ Desolvation Dictating Lithium-Ion Battery's Low-Temperature Performances," ACS Appl. Mater. Interfaces, **9**(49), pp. 42761–42768.

[10] Wu, H., and Cui, Y., 2012, "Designing Nanostructured Si Anodes for High Energy Lithium Ion Batteries," Nano Today, **7**(5), pp. 414–429.

[11] Yang, J., Li, J., Yang, Z., Liu, J., Xiang, Y., and Wu, F., 2022, "Self-Healing Silicon Anode via the Addition of GaInSn-Encapsulated Microcapsules," ACS Appl. Energy Mater., **5**(10), pp. 12945–12952.

[12] Li, X., Xu, C., Xia, T., Wang, C., Li, Z., Zhou, Y., Tang, Y., and Wu, P., 2022, "Integrating Transition Metal Into Silicon/Carbon Anodes Towards Enhanced Lithium Storage," J. Alloys Compd., **927**, p. 167085.

[13] Fang, K., Wang, M., Xia, Y., Li, J., Ji, Q., Yin, S., Xie, S., et al., 2017, "Facile Fabrication of Silicon Nanoparticle Lithium-Ion Battery Anode Reinforced With Copper Nanoparticles," Dig. J. Nanomater. Biostructures, **12**(2), pp. 243–253.

[14] Holoubek, J., Yu, M., Yu, S., Li, M., Wu, Z., Xia, D., Bhaladhare, P., et al., 2020, "An All-Fluorinated Ester Electrolyte for Stable High-Voltage Li Metal Batteries Capable of Ultra-Low-Temperature Operation," ACS Energy Lett., **5**(5), pp. 1438–1447.

[15] Holoubek, J., Liu, H., Wu, Z., Yin, Y., Xing, X., Cai, G., Yu, S., Zhou, H., Pascal, T. A., and Chen, Z., 2021, "Tailoring Electrolyte Solvation for Li Metal Batteries Cycled at Ultra-Low Temperature," Nat. Energy, **6**(3), pp. 303–313.

[16] Mennel, J. A., and Chidambaram, D., 2023, "A Review on the Development of Electrolytes for Lithium-Based Batteries for Low Temperature Applications," Front. Energy, **17**(1), pp. 1–29.

[17] Bachand, G., and Mennel, J., 2023, "Improved Performance of Silicon Anodes Using Copper Nanoparticles as Additive," ASME J. Electrochem. Energy Convers. Storage, **20**(4), p. 041009.

[18] Smart, M. C., Ratnakumar, B. V., Ewell, R. C., Surampudi, S., Puglia, F. J., and Gitzendanner, R., 2018, "The Use of Lithium-Ion Batteries for JPL's Mars Missions," Electrochim. Acta, **268**, pp. 27–40.

[19] Zhang, S. S., Xu, K., and Jow, T. R., 2003, "The Low Temperature Performance of Li-Ion Batteries," J. Power Sources, **115**(1), pp. 137–140.